

EXISTENCE AND UNIQUENESS OF RIGID-BODY DYNAMICS WITH COULOMB FRICTION

Pierre E. Dupont

Aerospace and Mechanical Engineering
 Boston University
 Boston, MA 02215 USA

ABSTRACT

For motion planning and verification, as well as for model-based control, it is important to have an accurate dynamic system model. In many cases, friction is a significant component of the model. When considering the solution of the rigid-body forward dynamics problem in systems such as robots, we can often appeal to the fundamental theorem of differential equations to prove the existence and uniqueness of the solution. It is known, however, that when Coulomb friction is added to the dynamic equations, the forward dynamic solution may not exist and if it exists, it is not necessarily unique. In these situations, the inverse dynamic problem is ill-posed as well. Thus there is the need to understand the nature of the existence and uniqueness problems and to know under what conditions these problems arise. In this paper, we show that even single degree of freedom systems can exhibit existence and uniqueness problems. Next, we introduce compliance in the otherwise rigid-body model. This has two effects. First, the forward and inverse problems become well-posed. Thus we are guaranteed unique solutions. Secondly, we show that the extra dynamic solutions associated with the rigid model are unstable.

1 INTRODUCTION

To plan motions, one needs to know what dynamic behavior will occur as the result of applying given forces or torques to the system. In addition, the simulation of motions is useful to verify motion planning operations. Alternatively, one may wish to design a feedforward controller which applies the forces or torques necessary to produce a desired output motion. Rigid-body models are often used for these tasks.

While frequently neglected, friction has been shown to be very significant in many systems. This applies both to friction between the rigid bodies making up the system [1,2,3] and to friction between the system and its environment [4]. In the context of this paper, the latter may constitute the most important case since the friction coefficient between a mechanism and its environment can be quite high. Robotic examples include the insertion of a peg into a hole and a finger sliding on an object surface prior to, or during, grasping.

Beginning at the turn of the century, a number of researchers have shown that when the simple Coulomb friction model is combined with the rigid-body forward dynamic equations, there are cases when no solutions exist [5] and also cases when multiple solutions occur [6,7,8].

In a recent paper, we have demonstrated that systems possessing a single degree of freedom can exhibit this behavior [9]. In these systems, existence and uniqueness problems arise only when the effective inertia of the system can take on a negative value. In this case, the value of input force or torque determines the number of solutions (0 – 3 for a single degree of freedom).

The question to be resolved is to determine if a unique motion can be associated with each value of input force or torque. The case of zero solutions has been successfully addressed in [5,9]. In the case of multiple solutions, it is easy to show that the static solution can be separated from the dynamic solutions [9]. What remains is to determine if the multiple dynamic solutions are all valid and, if so, which will occur. This problem has not been successfully addressed in the literature and is the topic of this paper.

In the next section, background material is presented and we describe the class of problems to be considered. In Section 3, the existence and uniqueness problem for systems with one degree of freedom is reviewed. In Section 4, we introduce compliant models and compare their dynamic equations with those of rigid-body models. A screw drive is used as an example. A stability analysis is given in Section 5 to show that the extra solutions from the scalar rigid-body model are unstable. Conclusions are presented in the final section of the paper.

2 BACKGROUND

The rigid-body dynamic equations for a mechanical system such as an open-kinematic-chain robot are of the form

$$\tau = A(q)\ddot{q} + b(q, \dot{q}) + f(q, \dot{q}, \ddot{q}). \quad (1)$$

The n -vectors of generalized coordinates (such as joint positions) and associated input forces or torques are q and τ , respectively where n is the number of degrees of freedom of the system. The configuration-dependent inertia matrix is represented by $A \in \mathbf{R}^{n \times n}$. It is both symmetric and positive definite. The vector $b \in \mathbf{R}^n$ consists of centrifugal, Coriolis and gravity terms. The vector $f \in \mathbf{R}^n$ includes all friction terms and is a function of the generalized coordinates and their first and second derivatives.

The Coulomb friction force is directed so as to oppose relative motion and is proportional to the normal force of contact during motion. For unilateral constraints, the normal force F_n must be positive and Coulomb friction can be expressed as

$$\begin{aligned} F_n &\geq 0 \\ v \neq 0 \Rightarrow |F_f| &= \mu F_n, \quad v F_f \leq 0 \\ v = 0 \Rightarrow |F_f| &\leq \mu F_n \end{aligned} \quad (2)$$

where F_f is friction force, $\mu > 0$ is the coefficient of friction and v is the velocity of relative motion. These equations define what is commonly called the friction cone. During motion, the friction force must lie on the friction cone while during static contact, it may also lie inside the cone.

The *forward dynamics problem* is to solve for the positions, velocities and accelerations given the input torques or forces and the initial conditions. This is the problem to be solved for simulation. At each time step, the known torques, positions and velocities are used to compute the accelerations. In the absence of friction, this involves solving a set of linear algebraic equations for the accelerations. Using the values of acceleration and velocity, numerical integration yields the velocity and position at the next time step. The *inverse dynamics problem* is simpler. Given the desired positions, velocities and accelerations, the system equation (1) is solved for the forces or torques at each instant of time. This is the approach taken in model-based control.

Friction can arise due to relative motion between the rigid bodies making up the mechanism or due to contact between one or more of these bodies and the environment. We will refer to these two types as *internal* and *external* friction, respectively. Internal friction is due to such elements as the transmissions and bearings. External friction acts at contacts between the robot and its environment. Thus, it is important in grasping and assembly operations.

In the case of external friction, (1) must be modified to include the Jacobian matrix relating infinitesimal joint and contact point displacements. If the generalized coordinate directions can be chosen so as to coincide with the directions of the external normal and friction forces then the Jacobian reduces to the identity matrix and the form of the expression reduces to (1). This is true in many important cases. We will only discuss problems of this type.

In general, the inclusion of load-dependent friction in the dynamic equations renders them implicit in the accelerations. The cause of the implicitness is the dependence of friction on the magnitude of the normal force which is itself a function of the resultant force at the frictional contact. Expressed in a local coordinate frame, the components of the resultant force can be formulated in terms of positions, velocities and accelerations. Just as with $\tau - f$ in (1), these components will be affine transformations of the accelerations.

If the direction of a normal force is constant in the local coordinate frame, the normal force can be expressed as an affine transformation of the joint accelerations [3]. For the case of a single source of friction associated with each degree of freedom, the friction vector, f , becomes

$$f(q, \dot{q}, \ddot{q}) = M|C(q)\ddot{q} + d(q, \dot{q})|. \quad (3)$$

Here $M \in \mathbf{R}^{n \times n}$ is a diagonal matrix with diagonal elements $\mu_i \operatorname{sgn}(\dot{q}_i)$ and $\mu_i > 0$ are the coefficients of friction. $C \in \mathbf{R}^{n \times n}$ takes the form of an inertia matrix and $d \in \mathbf{R}^n$. The expression in the absolute value is the normal force – an affine transformation of acceleration vector.

This expression is true, for example, of friction in transmissions, peg-in-hole insertion and sliding fingers. Since the sign of the normal force at a bilateral constraint can change, its absolute value must be used to obtain its magnitude [3]. Only friction of this form, (3), will be considered here.

3 EXISTENCE AND UNIQUENESS FOR THE SCALAR CASE

The scalar form of the dynamic equation (1), with friction of the form (3), is given by

$$a(q)\ddot{q} + b(q, \dot{q}) + \mu|c(q)\ddot{q} + d(q, \dot{q})|\operatorname{sgn}(\dot{q}) = \tau \quad (4)$$

Note that the single normal force, F_n , is given by $F_n = c\ddot{q} + d$. Thus we have two equations:

$$(a + \mu c)\ddot{q} + (b + \mu d) = \tau, \quad \operatorname{sgn}(\dot{q}) = \operatorname{sgn}(F_n) \quad (5)$$

$$(a - \mu c)\ddot{q} + (b - \mu d) = \tau, \quad \operatorname{sgn}(\dot{q}) \neq \operatorname{sgn}(F_n) \quad (6)$$

These equations are intersecting lines in the space formed by τ and \ddot{q} . From (4), it is clear that these lines depend on q and \dot{q} . For clarity of exposition, this dependency is neglected in the following discussion.

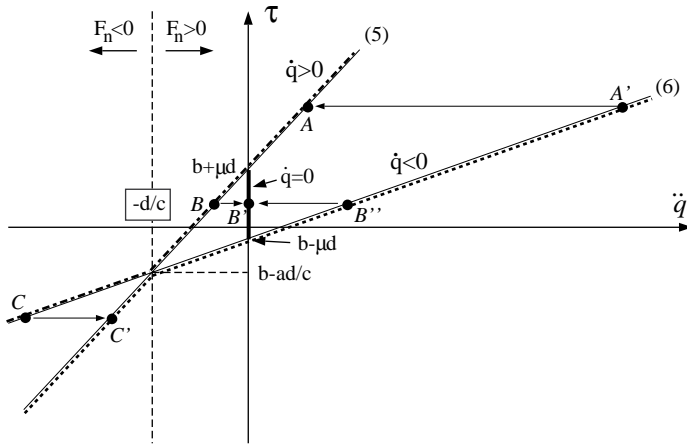


Figure 1: Scalar Case of τ Versus \dot{q} for $\mu < a/c$ and $d > 0$. Equations (5) and (6) form two V's. The upper, dot-dashed V corresponds to $\dot{q} > 0$. The lower, dotted V corresponds to $\dot{q} < 0$. The dark line segment on the τ -axis is the static region associated with $\dot{q} = 0$. The horizontal arrows indicate discontinuities in acceleration which occur when $\dot{q} = 0$.

3.1 SOLUTION EXISTS AND IS UNIQUE

The case of $\mu < a/c$ and $d > 0$ is shown in Figure 1. Note that a and c , representing inertias, must be positive. Since these equations represent bilateral constraints, normal force can be of either sign and $F_n = 0$ along the vertical line through $\dot{q} = -d/c$. Thus for $\dot{q} > 0$, the system lies on the upper V and for $\dot{q} < 0$, on the lower V. If the system is initially static, it lies on the τ axis between the two lines. From this static region, if the torque is increased above $b + \mu d$, motion with $\dot{q} > 0$ ensues. Similarly, if the torque is decreased below $b - \mu d$, motion with $\dot{q} < 0$ ensues. At $b \pm \mu d$, the friction force lies on the friction cone with $\dot{q} = 0$.

Consider the behavior of various points on the graph. At A , both the velocity and acceleration are positive. At B , acceleration is negative while the velocity is positive, but decreasing. Since point B is within the static band on the τ -axis, the system will stick when the velocity reaches zero. As shown by the arrow, the system jumps to B' and the acceleration discontinuously jumps to zero. Point C , however, is outside the static region. When $\dot{q} = 0$ is reached at C , the system jumps to C' on the negative-velocity V. For $\dot{q} < 0$, points B'' and A' lead to sticking and velocity reversal, respectively.

For almost all values of input torque, Figure 1, together with the current value of velocity, provides a unique value of acceleration. For example, consider that the three values of \dot{q} at B , B' and B'' are associated with a single value of torque. These solutions, however, correspond to $\dot{q} > 0$, $\dot{q} = 0$ and $\dot{q} < 0$, respectively. The two ambiguous points occur for $\tau = b \pm \mu d$. Note that a static friction coefficient, $\mu_s > \mu$, would resolve this ambiguity. Let us now consider the conditions under which solution existence and uniqueness fail for most values of input torque.

3.2 SOLUTION NONEXISTENCE AND MULTIPLICITY

Consider the graph of (5) and (6) in Figure 2. Here, $\mu > a/c$ and so (6) has a negative slope. This corresponds to a negative effective inertia. Once again, the upper V is associated with positive velocities and the lower with negative velocities. Starting from rest, the input torque must leave the static region to initiate motion. For example, if the torque is increased above $b + \mu d$, motion in the positive direction

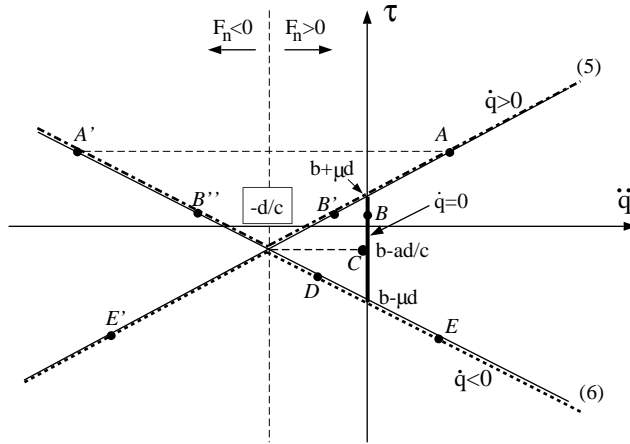


Figure 2: Scalar Case of τ Versus \dot{q} for $\mu > a/c$. In this case, there can be multiple solutions or none.

will ensue. Now, however, there are two possible solutions given, for example, by A and A' . If the torque is decreased to the value associated with B , there are three possible values of acceleration given by B , B' and B'' . B corresponds to the static case. B' and B'' both correspond to $\dot{q} > 0$, but with different values of acceleration, \ddot{q} .

If the torque is decreased slightly below $b - ad/c$, the only valid solution is the static case C , but as we saw with the previous figure, the system would normally only jump like this when the velocity reached zero. Thus, there appears to be no solution provided by the graph for $\dot{q} > 0$ and $\tau < (b - ad/c)$. We can make the same arguments for negative velocities. According to the value of input torque and velocity, we can have either zero, one, two or three feasible solutions.

In summary, a necessary and sufficient condition for solution existence and uniqueness for any value of input torque is given by

$$\mu < a/c \quad (7)$$

When $\mu \geq a/c$, there exists a critical value of torque, $\tau_{cr} = b - ad/c$, for which $\tau < \tau_{cr}$ yields no solutions and $\tau > \tau_{cr}$ yields two or three solutions (or vice versa depending on $\text{sgn}(\dot{q})$).

Several investigators have considered the case when $\dot{q} > 0$ and τ is decreased below $\tau_{cr} = b - ad/c$. They have concluded that velocity jumps discontinuously to zero. For an explanation, the reader is referred to [5] and [9]. Recently, the dynamics of this transition have been studied using compliant models [10].

In cases of multiple solutions such as given by B , B' and B'' in Figure 2, a method is needed to select the actual solution from the set of feasible solutions. We have already stated that the static case can only be escaped by applying a torque outside of the static region bounded by $b \pm \mu d$. Thus if \dot{q} is initially zero, B is the only possible solution. Solution pairs such as A , A' and B' , B'' , however, all correspond to $\dot{q} > 0$ and so velocity cannot be used to distinguish between them. This issue is resolved in the following sections by adding compliance to the model.

4 COMPLIANT-BODY MODELS

Recall that the definition of system state is such that if the state is known at time t_0 , the behavior of the system for $t > t_0$ can be computed given the inputs for $t \geq t_0$. For those cases when (7) is

not satisfied, however, specifying the position and velocity of the rigid bodies, (q, \dot{q}) , does not give a unique vector of accelerations, \ddot{q} , and thus the problem is ill-posed. The rigid-body formulation does not provide an adequate definition of system state.

To make the problem well-posed, we would like to add the minimum number of degrees of freedom to our state vector. Solution multiplicity arises due to the unknown sign of the normal force at the friction interface. Thus, our well-posed model must allow us to compute normal force as a function of system state.

To do so, we introduce nonzero compliance in the model. This is done by adding a spring with a component of its displacement along the direction of the normal force to the otherwise-rigid model. Any spring location is acceptable as long as the normal force can be expressed as a linear function of spring displacement. As a result, the sign of the normal force equals the sign of the spring displacement. In this way, we introduce one new degree of freedom (two new state variables, e.g., spring displacement and velocity) for each independent normal force.

4.1 DERIVATION OF RIGID AND COMPLIANT MODELS

To explain the equations associated with the compliant model, it is worthwhile to first explain in detail the derivation of the rigid model. The equations for the rigid-body model given by

$$a\ddot{q} + b + \mu|F_n|\text{sgn}(\dot{q}) = \tau \quad (8)$$

$$F_n = c\ddot{q} + d \quad (9)$$

are actually a simplified form. If one was to write the equations for the scalar system from a free-body analysis, two equations would be obtained.

$$a_1\ddot{q}_1 + b_1 + c_1F_n + \mu d_1|F_n|\text{sgn}(\dot{q}_r) = \tau_1 \quad (10)$$

$$a_2\ddot{q}_2 + b_2 + c_2F_n + \mu d_2|F_n|\text{sgn}(\dot{q}_r) = \tau_2 \quad (11)$$

In this form, the normal force can appear outside the absolute value and \dot{q}_r is the relative velocity at the friction interface.

4.1.1 RIGID-BODY ANALYSIS

In this case, the displacements q_1 and q_2 are related by a possibly nonlinear function

$$q_1 = g(q_2). \quad (12)$$

Choosing q_1 as the dependent variable, we can use (12) and its first two derivatives to solve (10) for F_n in terms of q_2 and its derivatives. This gives an expression of the form of (9).

4.1.2 COMPLIANT-BODY ANALYSIS

In this case, a spring is added to the system such that (12) is no longer satisfied. Instead, we can write an expression for normal force of the form

$$F_n = k_{eff}(q_1 - g(q_2)) \quad (13)$$

in which k_{eff} is the effective spring constant.

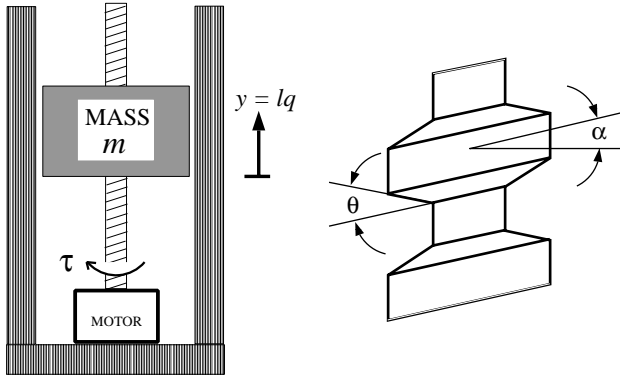


Figure 3: Screw-driven Mass. The motor applies torque τ to the screw. The mass, m , is attached to the nut. In the rigid case, its displacement, y , is related to the screw displacement, q , by the screw lead, l . The helix angle, α and thread angle, θ , are also shown.

With (12) no longer satisfied, q_1 and q_2 are now independent variables. We can substitute our expression for F_n into (10) and (11) to obtain the final form of these equations. Clearly, the sign of normal force is known, as is the relative velocity, and so the solution of these equations is a well-posed problem.

4.2 EXAMPLE: SCREW DRIVE

Screws are sometimes used as transmission elements in robots. See, for example, [3]. Consider the case of a screw moving a mass m with gravity acting downward as shown in Figure 3. The following definitions will be used.

$$\begin{array}{ll}
 q = \text{screw displacement (angle)} & y = \text{mass displacement} \\
 l = \text{screw lead (distance/angle)} & y = lq \\
 \alpha = \text{screw helix angle} & \theta = \text{screw thread angle} \\
 I = \text{rotational screw inertia} & \tan \rho = \mu / \cos \theta_n
 \end{array}$$

Summing forces on the screw and nut, we can obtain equations of the form given by (10) and (11). These are written in terms of the screw and mass displacements, q and y , respectively.

$$I\ddot{q} + \frac{l}{\tan \theta} (F_n \cos \theta \sin \alpha + |F_n| \mu \cos \alpha \operatorname{sgn}(\dot{q})) = \tau \quad (14)$$

$$m\ddot{y} - F_n \cos \theta \cos \alpha + |F_n| \mu \sin \alpha \operatorname{sgn}(\dot{q}) = -mg \quad (15)$$

4.2.1 RIGID-BODY ANALYSIS

If the screw and nut are rigid, the displacements q and y are related by the screw lead, l . Corresponding to (12), we have

$$y = lq \quad (16)$$

Selecting y as the dependent variable, we wish to obtain an expression for F_n like (9). Defining κ as

$$\kappa^2 = \mu^2 + \cos^2 \theta \quad (17)$$

(15) reduces to

$$m\ddot{y} - F_n \kappa^2 \cos(\alpha \pm \rho) = -mg \quad \begin{cases} + : \operatorname{sgn}(F_n) = \operatorname{sgn}(\dot{q}) \\ - : \operatorname{sgn}(F_n) \neq \operatorname{sgn}(\dot{q}) \end{cases} \quad (18)$$

Rearranging to get the form of (9),

$$F_n = \left(\frac{ml}{\kappa^2 \cos(\alpha \pm \rho)} \right) \ddot{q} + \frac{mg}{\kappa^2 \cos(\alpha \pm \rho)} \quad (19)$$

Note that the expression $\cos(\alpha \pm \rho)$ will be positive for friction coefficients satisfying

$$\mu < \frac{\cos \theta}{\tan \alpha} \quad (20)$$

Since θ and α are small angles, (20) can be true for very large coefficients of friction.

To obtain the final form of the rigid-body screw equations, (19) is substituted into (14). After simplification, the dynamic equation is found to be

$$\left(I + \frac{ml^2 \tan(\alpha \pm \rho)}{\tan \alpha} \right) \ddot{q} + \frac{mgl \tan(\alpha \pm \rho)}{\tan \alpha} = \tau \quad (21)$$

Introducing the standard expression, η_i , for screw efficiency,

$$\eta_i = \begin{cases} \eta_1 = \frac{\tan \alpha}{\tan(\alpha + \rho)}, & \operatorname{sgn}(F_n) = \operatorname{sgn}(\dot{q}) \\ \eta_2 = \frac{\tan \alpha}{\tan(\alpha - \rho)}, & \operatorname{sgn}(F_n) \neq \operatorname{sgn}(\dot{q}) \end{cases} \quad (22)$$

we can also write this as

$$\left(I + \frac{ml^2}{\eta_i} \right) \ddot{q} + \frac{mgl}{\eta_i} = \tau \quad (23)$$

4.2.2 COMPLIANT-BODY ANALYSIS

In this case, we need to add compliance to the screw/nut system such that a component of the spring displacement is parallel to the normal force. It is perhaps most appropriate to model the screw with both torsional and axial springs to represent screw twisting and stretching, respectively. Since the threads and hence, normal force, are inclined by the helix angle, both torsional and axial springs provide a component of displacement in the normal-force direction. For simplicity, let us consider only an axial spring as depicted in Figure 4.

Clearly, the springs impart a vertical force, F_v , on the nut given by

$$F_v = k(lq - y) \quad (24)$$

We can also express F_v as

$$F_v = m\ddot{y} + mg \quad (25)$$

Using (15), we can obtain an expression corresponding to (13).

$$F_n = \left(\frac{k}{\kappa^2 \cos(\alpha \pm \rho)} \right) (lq - y) \quad (26)$$

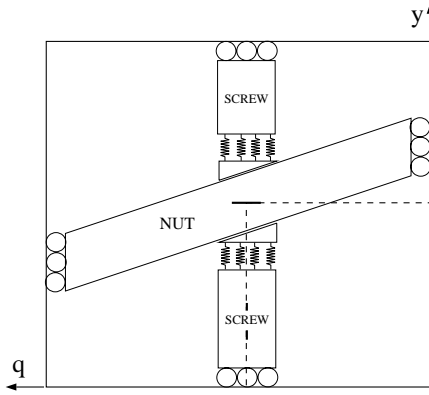


Figure 4: Planar Representation of Axially-compliant Screw Model. The springs are considered embedded in the screw adjacent to the friction interface. Physically, this might be construed as the stiffness of the screw and nut threads.

The variable sign is chosen as in the rigid-body case, but note that the effective stiffness is positive if (20) is satisfied. The sign of the normal force then depends on the sign of the spring displacement.

$$\operatorname{sgn}(F_n) = \operatorname{sgn}(lq - y) \quad (27)$$

The forward and inverse dynamics of (14) and (15) together with (26) are well posed. We can combine these three equations to obtain

$$I\ddot{q} + \frac{kl}{\eta_i}(lq - y) = \tau \quad (28)$$

$$m\ddot{y} - k(lq - y) = -mg \quad (29)$$

These two equations can be compared with the rigid-body equation (23). In this case, η_i is chosen according to $\operatorname{sgn}(lq - y) =, \neq \operatorname{sgn}(\dot{q})$.

5 STABILITY ANALYSIS

As discussed in Section 3, there are cases when the rigid-body formulation of the forward dynamics problem yields several possible values of acceleration for a fixed value of input torque. Examples are the pairs of points (A, A') , (B', B'') and (E, E') in Figure 2. These points are distinguished from each other by $\operatorname{sgn}(F_n)$.

Since, the compliant model provides a unique value of $\operatorname{sgn}(F_n)$, we can now pose the following questions: (1) Do corresponding multiple solutions exist for the compliant model? (2) If so, are they stable?

As the spring stiffness becomes very large, the compliant model approaches the rigid model. By considering this limiting case, it is possible to perform an approximate analysis. We can choose the stiffness large enough so that the dynamics affecting normal force will be fast, and the spring displacement small, compared to those affecting the coefficients $a_i(q)$, $b_i(q, \dot{q})$, $c_i(q)$ and $d_i(q)$ in equations (10) and (11). Thus, we can treat these coefficients as constants when considering the stability of the normal force dynamics. Put another way, we are considering the class of systems for which, in the time scale of interest, fixed values of input torque or force produce constant accelerations.

To answer question (1), consider that at each solution of the rigid-body equations, F_n is constant. For the compliant model, constant F_n implies that

$$q_1 - g(q_2) = \text{constant} \quad (30)$$

and therefore

$$\ddot{q}_1 = \ddot{g}(q_2) \quad (31)$$

Under the assumption that the coefficients a_i , b_i , c_i and d_i are constant over the time scale of interest, the rigid-body analysis which reduces (10) and (11) to (8) and (9) involves only the preceding equation. Therefore, the fixed points of the normal force dynamics for the compliant model correspond to the rigid-body solutions.

To answer question (2) regarding the stability of these fixed points, let us reformulate the problem. Recalling that (13) expresses the normal force of the compliant model, we can define a variable, v , expressing the (very small) spring displacement.

$$v = q_1 - g(q_2) \quad (32)$$

Differentiating this equation twice, we see that v evolves according to

$$\ddot{v} = \ddot{q}_1 - g_1(q_2)\ddot{q}_2 - g_2(q_2, \dot{q}_2) \quad (33)$$

As before, we assume that spring stiffness is large enough and thus v is small enough that we can evaluate g_1 and g_2 at the operating point of the slow dynamics.

Substituting (10) and (11) into (33) and expressing F_n in terms of v yields

$$\ddot{v} + kh_i v = u, \quad h_i = \begin{cases} h_1, & \text{sgn}(v) > 0 \\ h_2, & \text{sgn}(v) < 0 \end{cases} \quad (34)$$

in which h_1 , h_2 and u are constants and k is spring stiffness.

The fixed points of v correspond to the fixed points of normal force for the compliant model. Their stability depends upon the eigenvalues, λ , which satisfy the characteristic equation

$$\lambda^2 = -kh_i \quad (35)$$

Solutions are of the form

$$\begin{aligned} v &= c_1 \sin(\sqrt{kh_i}t) + c_2 \cos(\sqrt{kh_i}t) + u/kh_i, & h_i > 0 \\ v &= c_1 e^{\sqrt{kh_i}t} + c_2 e^{-\sqrt{kh_i}t} + u/kh_i, & h_i < 0 \end{aligned} \quad (36)$$

The former is the oscillatory solution expected from a compliant model without damping. The latter equation shows that if $h_i < 0$, the normal-force fixed point is unstable with the spring displacement, v , either increasing or decreasing exponentially according to initial conditions. An exponentially-increasing normal force would rapidly bring the system to rest under impact-like conditions. An exponentially-decreasing normal force would move the system towards the stable fixed point.

We have been considering the limiting case when $k \rightarrow \infty$ and the compliant model approaches the rigid model. From (36), it is clear that, in the limit, the particular solution for spring displacement goes to zero as expected. Now consider the addition of damping proportional to \dot{v} . (This is actually necessary to make the normal-force dynamics fast when $h_i > 0$.) For $h_i > 0$, the system will be stable and exhibit damped oscillations. For $h_i < 0$, however, no finite amount of damping will stabilize the system indicating that this case is not a valid solution of the rigid-body model.

5.1 EXAMPLE: SCREW DRIVE

Let us reconsider the screw example. The coefficients in (14) and (15) are, in fact, independent of q , y and their velocities. In this case, it is clear, without assumption, that the normal-force fixed points of the compliant model correspond to the rigid-body solutions. The spring displacement, from (24), is

$$v = lq - y \quad (37)$$

and we can use the compliant-model equations, (28) and (29), to solve

$$\ddot{v} = l\ddot{q} - \ddot{y} \quad (38)$$

These substitutions yield an expression of the form of (34).

$$\ddot{v} + k \left(\frac{I + ml^2/\eta_i}{mI} \right) v = (l/I)\tau + g \quad (39)$$

To determine stability, we are interested in the sign of h_i which, for this case, is

$$h_i = \left(\frac{I + ml^2/\eta_i}{mI} \right) \quad (40)$$

The sign of h_i depends on the sign of its numerator which is the effective inertia of the rigid-body model, (23). Recall from Section 3 that questions of existence and uniqueness arise when one solution gives a negative effective inertia. Therefore, we can associate $h_i > 0$ with normal-force fixed points corresponding to the positively-sloped line in Figure 2 and $h_i < 0$ with unstable fixed points corresponding to the negatively-sloped line.

Considering $\dot{q} > 0$ in Figure 2, this analysis tells us that for the pairs of solutions (A, A') and (B', B'') , the counterintuitive solutions, A' and B'' are unstable. This analysis also suggests that when initiating motion with $\dot{q} < 0$, \ddot{q} must jump discontinuously to the positively-sloped branch of E' .

6 CONCLUSIONS

In this paper, we have examined the effect of Coulomb friction on the forward and inverse dynamics of rigid-body systems. For the scalar case, we presented a necessary and sufficient condition for forward solution existence and uniqueness which was first derived in [9]. Violating this condition involves friction coefficients which exceed typical magnitudes of internal friction. This is an important result because it indicates that, in many cases, solution existence and uniqueness of both the forward and inverse dynamics is not problematic.

Coefficients of friction of this magnitude, however, may be encountered in certain low-efficiency transmissions and in external friction applications involving static or sliding contact with the environment. For these cases, it is important to understand the limitations of rigid-body models and to characterize the actual system motion. Toward this end, we have introduced a compliant-body formulation for which the normal force at the friction interface can be expressed as a function of system state.

The compliant-body model, while possessing an additional degree of freedom, leads to two results. First, this model does not exhibit the existence and uniqueness problems of the rigid-body model.

Secondly, the compliant-body model was used to analyze the multiple forward dynamic solutions of the rigid-body formulation. It was shown that the extra solution of the rigid-body model is unstable. By extending this technique to higher dimensional systems, it may be possible, even for high friction coefficients, to solve both forward and inverse dynamics problems using rigid-body models together with a set of stability rules for resolving the existence and uniqueness issues.

7 REFERENCES

1. Armstrong-Hélouvy, B., *Control of Machines with Friction*. Kluwer Academic Press, Boston, 1991.
2. Canudas De Wit, C. and Seront, V., "Robust Adaptive Friction Compensation." *Proceedings 1990 IEEE Int. Robotics and Automation Conf.*, Cincinnati, AZ, May 1990, pp. 1383-1388.
3. Dupont, P., "The Effect of Friction on the Forward Dynamics Problem." *International Journal of Robotics Research*, Vol. 12, No. 2, April 1993, pp. 164-79.
4. Kao, I. and Cutkosky, M., "Dextrous Manipulation with Compliance and Sliding." *The 5th International Symposium on Robotics Research*, MIT Press, August, 1989, pp. 375-382.
5. Mason, M. and Wang, Y., "On the Inconsistency of Rigid-body Frictional Planar Mechanics." *Proceedings 1988 IEEE Int. Robotics and Automation Conf.*, Philadelphia, PA, April, 1988, pp. 524-28.
6. Lötstedt, P., "Coulomb Friction in Two-dimensional Rigid Body Systems." *Zeitschrift für Angewandte Mathematik und Mechanik*, Vol. 61, 1981, pp. 605-615.
7. Painlevé, P., "Sur les Lois du Frottement de Glissement." *Comptes Rendus de l'Académie des Sciences*, Vol. 121, 1895, pp. 112-115.
8. Rajan, V., Burridge, R. and Schwartz, J., "Dynamics of a Rigid Body in Frictional Contact with Rigid Walls: Motion in Two Dimensions." *Proceedings 1987 IEEE Int. Robotics and Automation Conf.*, Raleigh, North Carolina, 1987, pp. 671-77.
9. Dupont, P., "The Effect of Coulomb Friction on the Existence and Uniqueness of the Forward Dynamics Problem." *Proceedings 1992 IEEE International Conference on Robotics and Automation*, Nice, France, May, 1992, pp. 1442-47.
10. Wang, Y.-T., Kumar, V. and Abel, J., "Dynamics of Rigid Bodies Undergoing Multiple Frictional Contacts." *Proceedings 1992 IEEE International Conference on Robotics and Automation*, Nice, France, May, 1992, pp. 2764-69.